

CHAPTER II

MATHEMATICAL AND NUMERICAL FORMULATION

In this chapter, a brief overview of the governing equations and the numerical discretization is given. This work is an extension of previous work in several fixed and rotary wing studies presented by Sankar et al [80, 81, 86-92]. The focus of this thesis is on the improvement of the hybrid method for rotors in forward flight. The present formulation requires solving the Navier-Stokes equations near the body and potential flow equations elsewhere.

2.1 Viscous Flow Formulation

2.1.1 Navier-Stokes Equations

The divergence form of Navier-Stokes equations is given by:

$$\frac{\partial \mathbf{q}}{\partial t} + \frac{\partial \mathbf{E}}{\partial x} + \frac{\partial \mathbf{F}}{\partial y} + \frac{\partial \mathbf{G}}{\partial z} = \frac{\partial \mathbf{R}}{\partial x} + \frac{\partial \mathbf{S}}{\partial y} + \frac{\partial \mathbf{T}}{\partial z} \quad (2.1)$$

where \mathbf{q} is the flow vector, \mathbf{E} , \mathbf{F} and \mathbf{G} are the inviscid flux vectors, \mathbf{R} , \mathbf{S} and \mathbf{T} are the viscous flux vectors.

$$\mathbf{q} = \begin{Bmatrix} \rho \\ \rho u \\ \rho v \\ \rho w \\ e \end{Bmatrix}$$

$$\mathbf{E}\vec{i} + \mathbf{F}\vec{j} + \mathbf{G}\vec{k} = \begin{Bmatrix} \rho \\ \rho u^2 + p \\ \rho uv \\ \rho uw \\ u(e + p) \end{Bmatrix} \vec{i} + \begin{Bmatrix} \rho \\ \rho uv \\ \rho v^2 + p \\ \rho vw \\ v(e + p) \end{Bmatrix} \vec{j} + \begin{Bmatrix} \rho \\ \rho uv \\ \rho vw \\ \rho w^2 + p \\ w(e + p) \end{Bmatrix} \vec{k} \quad (2.2)$$

$$\mathbf{R}\vec{i} + \mathbf{S}\vec{j} + \mathbf{T}\vec{k} = \begin{Bmatrix} 0 \\ \tau_{xx} \\ \tau_{yx} \\ \tau_{zx} \\ E_{x5} \end{Bmatrix} \vec{i} + \begin{Bmatrix} 0 \\ \tau_{xy} \\ \tau_{yy} \\ \tau_{zy} \\ E_{y5} \end{Bmatrix} \vec{j} + \begin{Bmatrix} 0 \\ \tau_{xz} \\ \tau_{yz} \\ \tau_{zz} \\ E_{z5} \end{Bmatrix} \vec{k}$$

Here ρ is the density; u , v , w are the Cartesian components of velocity, and p is the pressure. The quantity e is the total energy per unit volume and is given by:

$$e = \rho \left[C_V T + \frac{u^2 + v^2 + w^2}{2} \right] \quad (2.3)$$

where T is the temperature, and C_V is the specific heat at constant volume.

The stress terms are defined using Stokes hypothesis, assuming the bulk viscosity λ to be equal to $-2\mu/3$:

$$\begin{aligned} \tau_{xx} &= \frac{2}{3} \mu (2u_x - v_y - w_z) \\ \tau_{xy} &= \mu (u_y + v_x) \\ \tau_{xz} &= \mu (u_z + w_x) \\ \tau_{yy} &= \frac{2}{3} \mu (2v_y - u_x - w_z) \\ \tau_{yz} &= \mu (v_z + w_y) \\ \tau_{zz} &= \frac{2}{3} \mu (2w_z - u_x - v_y) \end{aligned}$$

$$\begin{aligned} E_{x5} &= u\tau_{xx} + v\tau_{xy} + w\tau_{xz} + k \frac{\partial T}{\partial x} \\ E_{y5} &= u\tau_{xy} + v\tau_{yy} + w\tau_{yz} + k \frac{\partial T}{\partial y} \\ E_{z5} &= u\tau_{xz} + v\tau_{yz} + w\tau_{zz} + k \frac{\partial T}{\partial z} \end{aligned} \quad (2.4)$$

where k is the thermal conductivity, related to the molecular viscosity through:

$$k = \frac{\mu C_P}{\text{Pr}} = \frac{\mu \gamma C_V}{\text{Pr}}$$

The local speed of sound is given by:

$$a = \sqrt{\gamma RT} = \sqrt{\gamma(\gamma - 1) \left[\frac{e}{\rho} - \frac{1}{2}(u^2 + v^2 + w^2) \right]} \quad (2.5)$$

Under the general transformation:

$$\begin{aligned} \xi &= \xi(x, y, z, t) \\ \eta &= \eta(x, y, z, t) \\ \zeta &= \zeta(x, y, z, t) \end{aligned} \quad (2.6)$$

Equation (2.1) may be re-expressed as [93]:

$$\hat{\mathbf{q}}_\tau + \hat{\mathbf{E}}_\xi + \hat{\mathbf{F}}_\eta + \hat{\mathbf{G}}_\zeta = (\hat{\mathbf{R}}_\xi + \hat{\mathbf{S}}_\eta + \hat{\mathbf{T}}_\zeta) \quad (2.7)$$

Here,

$$\hat{\mathbf{q}} = \frac{1}{J} \begin{Bmatrix} \rho \\ \rho u \\ \rho v \\ \rho w \\ e \end{Bmatrix} \quad (2.8)$$

J is the Jacobian of transformation given by:

$$J = \frac{1}{y_\xi(x_\zeta z_\eta - x_\eta z_\zeta) + y_\eta(x_\xi z_\zeta - x_\zeta z_\xi) + y_\zeta(x_\eta z_\xi - x_\xi z_\eta)} \quad (2.9)$$

The quantities $\hat{\mathbf{E}}, \hat{\mathbf{F}}, \hat{\mathbf{G}}$ and $\hat{\mathbf{R}}, \hat{\mathbf{S}}, \hat{\mathbf{T}}$ are related to their counter parts $\mathbf{E}, \mathbf{F}, \mathbf{G}, \mathbf{R}, \mathbf{S}$ and \mathbf{T} by:

$$\begin{aligned}
\hat{\mathbf{E}} &= \frac{1}{J} (\mathbf{E} \xi_x + \mathbf{F} \xi_y + \mathbf{G} \xi_z + \mathbf{q} \xi_t) \\
\hat{\mathbf{F}} &= \frac{1}{J} (\mathbf{E} \eta_x + \mathbf{F} \eta_y + \mathbf{G} \eta_z + \mathbf{q} \eta_t) \\
\hat{\mathbf{G}} &= \frac{1}{J} (\mathbf{E} \zeta_x + \mathbf{F} \zeta_y + \mathbf{G} \zeta_z + \mathbf{q} \zeta_t) \\
\hat{\mathbf{R}} &= \frac{1}{J} (\mathbf{R} \xi_x + \mathbf{S} \xi_y + \mathbf{T} \xi_z) \\
\hat{\mathbf{S}} &= \frac{1}{J} (\mathbf{R} \eta_x + \mathbf{S} \eta_y + \mathbf{T} \eta_z) \\
\hat{\mathbf{T}} &= \frac{1}{J} (\mathbf{R} \zeta_x + \mathbf{S} \zeta_y + \mathbf{T} \zeta_z)
\end{aligned} \tag{2.10}$$

where the quantity ξ_t, η_t and ζ_t are related to the velocity (x_τ, y_τ, z_τ) of the points in the physical domain (x, y, z) , as seen by an inertial observer, as:

$$\begin{aligned}
\xi_t &= -x_\tau \xi_x - y_\tau \xi_y - z_\tau \xi_z \\
\eta_t &= -x_\tau \eta_x - y_\tau \eta_y - z_\tau \eta_z \\
\zeta_t &= -x_\tau \zeta_x - y_\tau \zeta_y - z_\tau \zeta_z
\end{aligned} \tag{2.11}$$

The quantities ξ_x, ξ_y, ξ_z etc. are called the metrics of transformation and may be readily computed as shown in Ref. [93].

2.1.2 Numerical Discretization

The Navier-Stokes equations contain both spatial and temporal derivatives. These derivatives were approximated by numerical expressions as discussed below.

2.1.2.1 Temporal Discretization

Equation (2.7) can be written in semi-discrete form as:

$$\left. \frac{\partial \hat{\mathbf{q}}}{\partial t} \right|^{n+1} = - (\delta_\xi \hat{\mathbf{E}} + \delta_\eta \hat{\mathbf{F}} + \delta_\zeta \hat{\mathbf{G}}) \Big|^{n+1} + (\delta_\xi \hat{\mathbf{R}} + \delta_\eta \hat{\mathbf{S}} + \delta_\zeta \hat{\mathbf{T}}) \Big|^n \quad (2.12)$$

where, for example, $\delta_\xi \hat{\mathbf{E}}$ is a numerical approximation to the derivative $\partial \hat{\mathbf{E}} / \partial \xi$, to be discussed later. The superscripts refer to time levels ‘n’ and ‘n+1’.

The purpose of the Navier-Stokes solver is to advance the solution from one time step ‘n’ to the next ‘n+1’. This is done using a semi-implicit time marching scheme. In the present work, the time derivative is written as:

$$\left. \frac{\partial \hat{\mathbf{q}}}{\partial t} \right|^{n+1} = \frac{\hat{\mathbf{q}}^{n+1} - \hat{\mathbf{q}}^n}{\Delta t} + O(\Delta t) \quad (2.13)$$

This yields:

$$\hat{\mathbf{q}}^{n+1} = \hat{\mathbf{q}}^n - \Delta t(\delta_\xi \hat{\mathbf{E}}^{n+1} + \delta_\eta \hat{\mathbf{F}}^{n+1} + \delta_\zeta \hat{\mathbf{G}}^{n+1}) + \Delta t(\delta_\xi \hat{\mathbf{R}}^n + \delta_\eta \hat{\mathbf{S}}^n + \delta_\zeta \hat{\mathbf{T}}^n) \quad (2.14)$$

The above discretization yields a nonlinear system of algebraic equations for the unknown flow properties $\hat{\mathbf{q}}$ at the time level 'n+1'. Following Beam and Warming [94], the nonlinear fluxes are linearized as:

$$\begin{aligned} \hat{\mathbf{E}}^{n+1} &= \hat{\mathbf{E}}^n + \left(\frac{\partial \hat{\mathbf{E}}}{\partial \hat{\mathbf{q}}} \right)^n \Delta \hat{\mathbf{q}}^n + O(\Delta t^2) \\ \hat{\mathbf{E}}^{n+1} &= \hat{\mathbf{E}}^n + \mathbf{A}^n \Delta \hat{\mathbf{q}}^n \\ \hat{\mathbf{F}}^{n+1} &= \hat{\mathbf{F}}^n + \left(\frac{\partial \hat{\mathbf{F}}}{\partial \hat{\mathbf{q}}} \right)^n \Delta \hat{\mathbf{q}}^n + O(\Delta t^2) \\ \hat{\mathbf{F}}^{n+1} &= \hat{\mathbf{F}}^n + \mathbf{B}^n \Delta \hat{\mathbf{q}}^n \\ \hat{\mathbf{G}}^{n+1} &= \hat{\mathbf{G}}^n + \left(\frac{\partial \hat{\mathbf{G}}}{\partial \hat{\mathbf{q}}} \right)^n \Delta \hat{\mathbf{q}}^n + O(\Delta t^2) \\ \hat{\mathbf{G}}^{n+1} &= \hat{\mathbf{G}}^n + \mathbf{C}^n \Delta \hat{\mathbf{q}}^n \end{aligned} \quad (2.15)$$

where

$$\Delta \hat{\mathbf{q}}^n = \hat{\mathbf{q}}^{n+1} - \hat{\mathbf{q}}^n$$

The quantities:

$$\begin{aligned}
\mathbf{A} &= \frac{\partial \hat{\mathbf{E}}}{\partial \hat{\mathbf{q}}} \\
\mathbf{B} &= \frac{\partial \hat{\mathbf{F}}}{\partial \hat{\mathbf{q}}} \\
\mathbf{C} &= \frac{\partial \hat{\mathbf{G}}}{\partial \hat{\mathbf{q}}}
\end{aligned} \tag{2.16}$$

are the flux Jacobians. These are 5x5 matrices and are given in classical CFD textbooks [93] and by Chaussee [95] and Pulliam [96]. The detailed form of these matrices is shown below (the matrix \mathbf{K} is \mathbf{A} or \mathbf{B} or \mathbf{C} when k is taken to be ξ or η or ζ):

$$\mathbf{K} = \begin{bmatrix} k_t & k_x & k_y & k_z & 0 \\ k_x \phi^2 - u\theta & \Theta - k_x(\gamma - 2)u & k_y u - \sigma k_x v & k_z u - \sigma k_x w & k_x \sigma \\ k_y \phi^2 - v\theta & k_x v - \sigma k_y u & \Theta - k_y(\gamma - 2)v & k_z v - \sigma k_y w & k_y \sigma \\ k_z \phi^2 - w\theta & k_x w - \sigma k_z u & k_y w - \sigma k_z v & \Theta - k_z(\gamma - 2)w & k_z \sigma \\ \theta(\phi^2 - E) & k_x E - \sigma u \theta & k_y E - \sigma v \theta & k_z E - \sigma w \theta & k_t + \sigma \theta \end{bmatrix} \tag{2.17}$$

where:

$$\begin{aligned}
\phi^2 &= (\gamma - 1)(u^2 + v^2 + w^2) / 2 \\
\theta &= k_x u + k_y v + k_z w \\
\sigma &= \gamma - 1 \\
\Theta &= k_t + \theta \\
E &= \frac{\gamma e}{\rho} - \phi^2
\end{aligned} \tag{2.18}$$

Following the linearization, the equation (2.14) can be written as a set of linear, algebraic equations:

$$\left[\mathbf{I} + \Delta t (\delta_\xi \mathbf{A}^n + \delta_\eta \mathbf{B}^n + \delta_\zeta \mathbf{C}^n) \right] \Delta \hat{\mathbf{q}}^{n+1} = \mathbf{RHS}^n \quad (2.19)$$

where the term **RHS**, sometimes referred to as the residual, is given by:

$$\mathbf{RHS}^n = -\Delta t (\delta_\xi \hat{\mathbf{E}}^n + \delta_\eta \hat{\mathbf{F}}^n + \delta_\zeta \hat{\mathbf{G}}^n) + \Delta t (\delta_\xi \hat{\mathbf{R}}^n + \delta_\eta \hat{\mathbf{S}}^n + \delta_\zeta \hat{\mathbf{T}}^n) \quad (2.20)$$

If classical finite difference methods are used to discretize the matrix form on the left hand side, a seven-diagonal equation will result which is costly to invert. The approximate factorization scheme by Beam and Warming [94] was used in the present study to avoid inverting the block seven diagonal matrix:

$$\left[\mathbf{I} + \Delta t (\delta_\xi \mathbf{A} + \delta_\eta \mathbf{B} + \delta_\zeta \mathbf{C}) \right] \cong \left[\mathbf{I} + \Delta t (\delta_\xi \mathbf{A}) \right] \left[\mathbf{I} + \Delta t (\delta_\eta \mathbf{B}) \right] \left[\mathbf{I} + \Delta t (\delta_\zeta \mathbf{C}) \right] + o(\Delta t^2) \quad (2.21)$$

If the operators $\delta_\xi (\mathbf{A} \Delta \hat{\mathbf{q}})$ etc. are evaluated using symmetric differences such as:

$$\delta_\xi (\mathbf{A} \Delta \hat{\mathbf{q}}) = \frac{(\mathbf{A} \Delta \hat{\mathbf{q}})_{i+1} - (\mathbf{A} \Delta \hat{\mathbf{q}})_{i-1}}{2\Delta \xi} \quad (2.22)$$

then it is likely that high frequency spatial oscillations will arise in $\Delta \hat{\mathbf{q}}$. Implicit second order low pass filter terms are introduced to alleviate this error [88].

The equation (2.20) may be solved by the three step process:

$$\begin{aligned}
[\mathbf{I} + \Delta t(\delta_\xi \mathbf{A}^n) - \Delta t \varepsilon_1 \nabla_\xi \phi_1 \Delta_\xi] \Delta \hat{\mathbf{q}}^{**} &= \mathbf{RHS}^n \\
[\mathbf{I} + \Delta t(\delta_\eta \mathbf{B}^n) - \Delta t \varepsilon_1 \nabla_\eta \phi_2 \Delta_\eta] \Delta \hat{\mathbf{q}}^* &= \Delta \hat{\mathbf{q}}^{**} \\
[\mathbf{I} + \Delta t(\delta_\zeta \mathbf{C}^n) - \Delta t \varepsilon_1 \nabla_\zeta \phi_3 \Delta_\zeta] \Delta \hat{\mathbf{q}}^{n+1} &= \Delta \hat{\mathbf{q}}^*
\end{aligned} \tag{2.23}$$

Here, ϕ_i is a low pass filter coefficient based on the spectral radius of the flux Jacobian matrix \mathbf{A} , \mathbf{B} or \mathbf{C} , respectively. Pulliam and Chaussee [97] showed further computational reductions with a diagonal form of the Alternating Direction Implicit (ADI) factorization scheme. They first expressed the matrices \mathbf{A} , \mathbf{B} and \mathbf{C} using the similarity transformation as:

$$\begin{aligned}
\mathbf{A} &= \mathbf{T}_\xi \mathbf{\Lambda}_\xi \mathbf{T}_\xi^{-1} \\
\mathbf{B} &= \mathbf{T}_\eta \mathbf{\Lambda}_\eta \mathbf{T}_\eta^{-1} \\
\mathbf{C} &= \mathbf{T}_\zeta \mathbf{\Lambda}_\zeta \mathbf{T}_\zeta^{-1}
\end{aligned} \tag{2.24}$$

where $\mathbf{\Lambda}_\xi$, $\mathbf{\Lambda}_\eta$ and $\mathbf{\Lambda}_\zeta$ are diagonal matrices defined as:

$$\begin{aligned}
\mathbf{\Lambda}_\xi &= \text{diag}(U, U, U, U + a\sqrt{\xi_x^2 + \xi_y^2 + \xi_z^2}, U - a\sqrt{\xi_x^2 + \xi_y^2 + \xi_z^2}) \\
\mathbf{\Lambda}_\eta &= \text{diag}(V, V, V, V + a\sqrt{\eta_x^2 + \eta_y^2 + \eta_z^2}, V - a\sqrt{\eta_x^2 + \eta_y^2 + \eta_z^2}) \\
\mathbf{\Lambda}_\zeta &= \text{diag}(W, W, W, W + a\sqrt{\zeta_x^2 + \zeta_y^2 + \zeta_z^2}, W - a\sqrt{\zeta_x^2 + \zeta_y^2 + \zeta_z^2})
\end{aligned} \tag{2.25}$$

where the contravariant velocities U , V , W are given as:

$$\begin{aligned}
U &= \xi_t + \xi_x u + \xi_y v + \xi_z w \\
V &= \eta_t + \eta_x u + \eta_y v + \eta_z w \\
W &= \zeta_t + \zeta_x u + \zeta_y v + \zeta_z w
\end{aligned} \tag{2.26}$$

The matrix \mathbf{T}_k is \mathbf{T}_ξ or \mathbf{T}_η or \mathbf{T}_ζ when k is taken to be ξ or η or ζ . The matrix \mathbf{T}_k and its inverse are given below:

$$\mathbf{T}_k = \begin{bmatrix} \tilde{k}_x & \tilde{k}_y & \tilde{k}_z & \alpha & \alpha \\ \tilde{k}_x u & \tilde{k}_y u - \tilde{k}_z \rho & \tilde{k}_z u + \tilde{k}_y \rho & \alpha(u + \tilde{k}_x a) & \alpha(u - \tilde{k}_x a) \\ \tilde{k}_x v + \tilde{k}_z \rho & \tilde{k}_y v & \tilde{k}_z v - \tilde{k}_x \rho & \alpha(v + \tilde{k}_y a) & \alpha(v - \tilde{k}_y a) \\ \tilde{k}_x w - \tilde{k}_y \rho & \tilde{k}_y w + \tilde{k}_x \rho & \tilde{k}_z w & \alpha(w + \tilde{k}_z a) & \alpha(w - \tilde{k}_z a) \\ t_{k5x} & t_{k5y} & t_{k5z} & \alpha \left[\frac{\phi^2 + a^2}{\gamma - 1} + a\tilde{\theta} \right] & \alpha \left[\frac{\phi^2 + a^2}{\gamma - 1} - a\tilde{\theta} \right] \end{bmatrix}$$

$$\mathbf{T}_k^{-1} = \begin{bmatrix} \tilde{k}_x f - \rho^{-1}(\tilde{k}_z v - \tilde{k}_y w) & \tilde{k}_x u g & \tilde{k}_x v g + \tilde{k}_z \rho^{-1} & \tilde{k}_x w g - \tilde{k}_y \rho^{-1} & -\tilde{k}_x g \\ \tilde{k}_y f - \rho^{-1}(\tilde{k}_x w - \tilde{k}_z u) & \tilde{k}_y u g - \tilde{k}_z \rho^{-1} & \tilde{k}_y v g & \tilde{k}_y w g + \tilde{k}_x \rho^{-1} & -\tilde{k}_y g \\ \tilde{k}_z f - \rho^{-1}(\tilde{k}_y u - \tilde{k}_x v) & \tilde{k}_z u g + \tilde{k}_y \rho^{-1} & \tilde{k}_z v g - \tilde{k}_x \rho^{-1} & \tilde{k}_z w g & -\tilde{k}_z g \\ \beta(\phi^2 - a\tilde{\theta}) & \beta(\tilde{k}_x a - \gamma_1 u) & \beta(\tilde{k}_y a - \gamma_1 v) & \beta(\tilde{k}_z a - \gamma_1 w) & \beta\gamma_1 \\ \beta(\phi^2 + a\tilde{\theta}) & -\beta(\tilde{k}_x a + \gamma_1 u) & -\beta(\tilde{k}_y a + \gamma_1 v) & -\beta(\tilde{k}_z a + \gamma_1 w) & \beta\gamma_1 \end{bmatrix} \tag{2.27}$$

where:

$$\tilde{k}_{x,y,z} = \frac{k_{x,y,z}}{\sqrt{k_x^2 + k_y^2 + k_z^2}};$$

$$\phi = (\gamma - 1)(u^2 + v^2 + w^2) / 2;$$

$$\begin{aligned}
\alpha &= \frac{\rho}{\sqrt{2a}}; \\
\tilde{\theta} &= \tilde{k}_x u + \tilde{k}_y v + \tilde{k}_z w; \\
t_{k5x} &= \tilde{k}_x \frac{\phi^2}{\gamma-1} + \rho(\tilde{k}_z v - \tilde{k}_y w); \\
t_{k5y} &= \tilde{k}_y \frac{\phi^2}{\gamma-1} + \rho(\tilde{k}_x w - \tilde{k}_z u); \\
t_{k5z} &= \tilde{k}_z \frac{\phi^2}{\gamma-1} + \rho(\tilde{k}_y u - \tilde{k}_x v); \\
\beta &= \frac{1}{\sqrt{2\rho a}}; \\
\gamma_1 &= \gamma - 1; \\
f &= (1 - \phi^2 / a^2); \\
g &= (\gamma - 1) / a^2
\end{aligned} \tag{2.28}$$

The diagonal form of equation (2.19) can be written before the inclusion of the low pass filter as:

$$\mathbf{T}_\xi^n [\mathbf{I} + \Delta t \delta_\xi \mathbf{\Lambda}_\xi^n] (\mathbf{T}_\xi^{-1} \mathbf{T}_\eta)^n [\mathbf{I} + \Delta t \delta_\eta \mathbf{\Lambda}_\eta^n] (\mathbf{T}_\eta^{-1} \mathbf{T}_\zeta)^n [\mathbf{I} + \Delta t \delta_\zeta \mathbf{\Lambda}_\zeta^n] (\mathbf{T}_\zeta^{-1})^n \Delta \mathbf{q}^{n+1} \cong \mathbf{RHS}^n \tag{2.29}$$

Equation (2.29) may be solved (after adding the low pass filters) using the following three-step process:

$$\begin{aligned}
[\mathbf{I} + \Delta t(\delta_\xi \mathbf{\Lambda}_\xi^n) - \Delta t \delta_\xi \lambda_1 \delta_\xi] \Delta \hat{\mathbf{q}}^* &= (\mathbf{T}_\xi^{-1})^n \mathbf{RHS}^n \\
[\mathbf{I} + \Delta t(\delta_\eta \mathbf{\Lambda}_\eta^n) - \Delta t \delta_\eta \lambda_2 \delta_\eta] \Delta \hat{\mathbf{q}}^{**} &= (\mathbf{T}_\xi \mathbf{T}_\eta^{-1})^n \Delta \hat{\mathbf{q}}^* \\
[\mathbf{I} + \Delta t(\delta_\zeta \mathbf{\Lambda}_\zeta^n) - \Delta t \delta_\zeta \lambda_3 \delta_\zeta] \Delta \hat{\mathbf{q}}^{***} &= (\mathbf{T}_\eta \mathbf{T}_\zeta^{-1})^n \Delta \hat{\mathbf{q}}^{**} \\
\Delta \hat{\mathbf{q}}^{n+1} &= (\mathbf{T}_\zeta)^n \Delta \hat{\mathbf{q}}^{***}
\end{aligned} \tag{2.30}$$

Once $\Delta \hat{\mathbf{q}}^{n+1}$ is known, the flow properties at the new time level may be written

as:

$$\hat{\mathbf{q}}^{n+1} = \left(\frac{\mathbf{q}}{J} \right)^{n+1} = \left(\frac{\mathbf{q}}{J} \right)^n + \Delta \hat{\mathbf{q}}^{n+1} \tag{2.31}$$

2.1.2.2 Spatial Discretization of the Inviscid Terms

The right hand side of equation (2.29) contains terms such as $\delta_\xi \hat{E}$, where \hat{E} has the interpretation of the flux of mass, momentum and energy. This flux is caused by upstream and downstream traveling acoustic, entropy and vortical waves and must be appropriately computed. The most popular methods for computing the fluxes are the Van Leer's flux-vector splitting [98-100], and Roe's flux-difference splitting [101,102] schemes.

Roe's approximate Riemann solver is used in the present work. It is given by:

$$\delta_{\xi} \hat{\mathbf{E}} = \frac{\bar{\mathbf{E}}_{i+1/2,j,k} - \bar{\mathbf{E}}_{i-1/2,j,k}}{\Delta \xi} \quad (2.32)$$

where (i, j, k) is a typical node, and $\bar{\mathbf{E}}$ is the numerical flux:

$$\bar{\mathbf{E}}_{i+1/2,j,k} = 0.5 \left\{ (\hat{\mathbf{E}}_L + \hat{\mathbf{E}}_R) - |\hat{\mathbf{A}}| (\hat{\mathbf{q}}_R - \hat{\mathbf{q}}_L) \right\} \quad (2.33)$$

Here, $|\hat{\mathbf{A}}| = \left| \partial \hat{\mathbf{E}} / \partial \hat{\mathbf{q}} \right| = \mathbf{T} |\mathbf{\Lambda}| \mathbf{T}^{-1}$, assuming $\hat{\mathbf{A}} = \mathbf{T} \mathbf{\Lambda} \mathbf{T}^{-1}$.

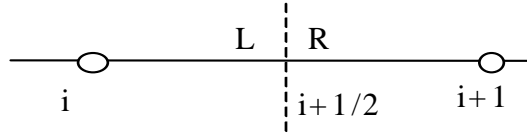


Figure 2.1: Grid Nodes and Cell Surface

The quantities $\hat{\mathbf{E}}_L$ and $\hat{\mathbf{E}}_R$ are fluxes $\hat{\mathbf{E}}$, evaluated at the node (i+1/2,j,k) using the information to the left and right of the node i+1/2.

The quantity $|\hat{\mathbf{A}}| (\hat{\mathbf{q}}_R - \hat{\mathbf{q}}_L)$ may be analytically expressed as follows:

$$|\hat{\mathbf{A}}|(\hat{\mathbf{q}}_R - \hat{\mathbf{q}}_L) = |\tilde{\lambda}_1| \begin{Bmatrix} \Delta\rho \\ \Delta\rho u \\ \Delta\rho v \\ \Delta\rho w \\ \Delta e \end{Bmatrix} + \delta_1 \begin{Bmatrix} \tilde{\rho} \\ \tilde{\rho}\tilde{u} \\ \tilde{\rho}\tilde{v} \\ \tilde{\rho}\tilde{w} \\ \tilde{\rho}\tilde{h} \end{Bmatrix} + \delta_2 \begin{Bmatrix} 0 \\ n_x \\ n_y \\ n_z \\ \tilde{U}_c \end{Bmatrix} \quad (2.34)$$

where

$$\begin{aligned} \delta_1 &= C_1 \frac{\Delta\rho}{\tilde{\rho}\tilde{c}^2} + 0.5C_2 \frac{\Delta U_c}{\tilde{c}} \\ \delta_2 &= C_1 \tilde{\rho} \Delta U_c - 0.5C_2 \frac{\Delta p}{\tilde{c}} \\ C_1 &= -|\tilde{\lambda}_1| + 0.5(|\tilde{\lambda}_2| + |\tilde{\lambda}_3|) \\ C_2 &= |\tilde{\lambda}_2| - |\tilde{\lambda}_3| \end{aligned} \quad (2.35)$$

The characteristic wave speeds and the contravariant velocity \tilde{U}_c are defined by

$$\begin{aligned} \tilde{\lambda}_1 &= \tilde{U} ; \quad \tilde{\lambda}_2 = \tilde{U} + \tilde{c} ; \quad \tilde{\lambda}_3 = \tilde{U} - \tilde{c} \\ \tilde{U}_c &= (\tilde{u}\vec{i} + \tilde{v}\vec{j} + \tilde{w}\vec{k}) \cdot (n_x\vec{i} + n_y\vec{j} + n_z\vec{k}) \end{aligned} \quad (2.36)$$

and

$$n_x\vec{i} + n_y\vec{j} + n_z\vec{k} = \frac{\vec{\nabla}\xi}{J} \quad (2.37)$$

This vector may be thought of as a unit normal vector to the surface $\xi=\text{constant}$ times a cell face area associated with the halfnode $(i+1/2, j, k)$.

All the flow quantities with ‘~’ represent the Roe-averaged quantities that are defined for any given flow variable ϕ other than ρ as:

$$\begin{aligned}\tilde{\rho} &= \sqrt{\rho_R \rho_L} \\ \tilde{\phi} &= \phi_L \left(\frac{1}{1 + \sqrt{\rho_R / \rho_L}} \right) + \phi_R \left(\frac{\sqrt{\rho_R / \rho_L}}{1 + \sqrt{\rho_R / \rho_L}} \right)\end{aligned}\quad (2.38)$$

The accuracy with which primitive variable field, \mathbf{q} , at the nodes $(i \pm 1/2, j, k)$ is evaluated determines the spatial accuracy of the solution [99]. A one-parameter family of interpolated values for the left state at the $i+1/2$ face and the right state at the $i+1/2$ face can be written as:

$$\begin{aligned}\mathbf{q}_L &= \{1 + [(1-k)\nabla + (1+k)\Delta]/4\} \mathbf{q}_i \\ \mathbf{q}_R &= \{1 - [(1+k)\nabla + (1-k)\Delta]/4\} \mathbf{q}_{i+1}\end{aligned}\quad (2.39)$$

The choice for k determines the spatial accuracy of the reconstruction. For example, $k=0$ yields first-order accuracy, while $k=1$ yields second-order accuracy. If $k=1/3$, a third-order upwind scheme results. This variable extrapolation method is called the Monotonic Upstream-centered Scheme for Conservation Laws (MUSCL). In the hybrid solver, a fifth-order ENO scheme is also available to calculate the inviscid fluxes [49]. A fixed stencil approximation is used to compute \mathbf{q}_L at cell face $(i+1/2, j, k)$ with nodes $i-2, i-1, i, i+1, i+2$ and \mathbf{q}_R with nodes $i-1, i, i+1, i+2, i+3$.

In regions with large gradients (such as shocks), the high-order interpolation term must be reduced to a lower order to maintain stability and to eliminate numerical oscillations in the solution. Limiters are designed by altering the high-order term to yield interface reconstructions which are within the bounds of the adjacent cell averages. A primitive variable limiting model is applied to the forward and backward gradients of the primitive variables:

$$\begin{aligned}\mathbf{q}_L &= \{1 + \phi^l [(1 - \phi^l k) \nabla + (1 + \phi^l k) \Delta] / 4\} \mathbf{q}_i \\ \mathbf{q}_R &= \{1 + \phi^r [(1 + \phi^r k) \nabla + (1 - \phi^r k) \Delta] / 4\} \mathbf{q}_{i+1}\end{aligned}\tag{2.40}$$

Here ϕ^l and ϕ^r are designed so that they go to zero in the vicinity of discontinuities. Venkatakrishnan's limiter [103] is designed to control the balance between convergence, accuracy and monotonicity. It was used in the present work:

$$\begin{aligned}\phi^l &= \frac{(\Delta q_i)^2 + 2\Delta q_i \nabla q_i + \varepsilon}{(\Delta q_i)^2 + 2(\nabla q_i)^2 + \Delta q_i \nabla q_i + \varepsilon} \\ \phi^r &= \frac{(\nabla q_{i+1})^2 + 2\Delta q_{i+1} \nabla q_{i+1} + \varepsilon}{2(\Delta q_{i+1})^2 + (\nabla q_{i+1})^2 + \Delta q_{i+1} \nabla q_{i+1} + \varepsilon}\end{aligned}\tag{2.41}$$

where ε is a non-vanishing parameter and is an input parameter.

2.1.2.3 Discretization of the Viscous Terms

A typical term such as $\delta_\xi \hat{\mathbf{R}}$ is written as $(\hat{\mathbf{R}}_{i+1/2} - \hat{\mathbf{R}}_{i-1/2})/\Delta\xi$. $\hat{\mathbf{R}}$ itself may contain additional derivatives such as $\frac{\partial u}{\partial x}$. These are expressed as:

$$\frac{\partial u}{\partial x} = \frac{\partial u}{\partial \xi} \xi_x + \frac{\partial u}{\partial \eta} \eta_x + \frac{\partial u}{\partial \zeta} \zeta_x \quad (2.42)$$

The derivatives are computed using standard central differences. For example,

$$\left. \frac{\partial u}{\partial \xi} \right|_{i+1/2, j, k} = \frac{u_{i+1} - u_i}{\Delta\xi} \quad (2.43)$$

The matrices needed at the half point are directly calculated.

2.1.2.4 Eddy Viscosity Model

While solving the Reynolds-averaged Navier-Stokes equations, when computing the viscous fluxes, it is necessary to make a closure assumption about the Reynolds stress and the heat flux quantities. The algebraic Baldwin-Lomax turbulence model is used in the present method for simplicity. This is a two-layer algebraic model. In the inner layer close the wall, the eddy viscosity μ_T is given by:

$$(\mu_T)_{innerlayer} = \rho l_m^2 |\omega| \quad (2.44)$$

where l_m is the mixing length modified by the Prandtl-Van Driest damping factor as shown below:

$$l_m = \kappa z \left\{ 1 - \exp\left(\frac{-z\rho_w\tau_w}{26\mu_w}\right) \right\} \quad (2.45)$$

Here, κ is the Von Karman constant, set to 0.4. The quantity z represents the physical distance from the nearest wall.

The local vorticity ω is defined as:

$$|\omega| = \sqrt{\left(\frac{\partial w}{\partial y} - \frac{\partial v}{\partial z}\right)^2 + \left(\frac{\partial u}{\partial z} - \frac{\partial w}{\partial x}\right)^2 + \left(\frac{\partial v}{\partial x} - \frac{\partial u}{\partial y}\right)^2} \quad (2.46)$$

In the outer layer, the eddy viscosity is calculated as:

$$(\mu_T)_{outerlayer} = K_c C_{cp} \rho F_{wake} F_{kleb} \quad (2.47)$$

where:

$$F_{wake} = \min\left(z_{\max} F_{\max}, \frac{0.25z_{\max} U_{dif}^2}{F_{\max}}\right)$$

$$F(z) = z|\omega| \left(1 - \exp\left(\frac{-z\rho_w\tau_w}{26\mu_w}\right)\right) \quad (2.48)$$

$$U_{dif} = \left(\sqrt{u^2 + v^2 + w^2}\right)_{\max} - \left(\sqrt{u^2 + v^2 + w^2}\right)_{\min}$$

$$F_{kleb} = \frac{1}{1 + 5.5 \left(\frac{0.3z}{z_{max}} \right)^6}$$

The constant $K_c = 0.0168$ is the Clauser's constant, and $C_{cp} = 1.6$ is an empirical constant. The Klebanoff intermittency correction, F_{kleb} , and the function F_{wake} are based on a formulation by Cebeci [104], and drive the eddy viscosity to zero far away from solid walls.

2.2 Potential Flow Formulation

2.2.1 Potential Flow Equations

In the present method, inviscid flow equations are solved away from the viscous regions. In the inviscid region, the mass conservation equation is solved with a velocity decomposition:

$$\rho_t + \nabla \cdot \rho \vec{V} = 0 \quad (2.49)$$

The velocity is assumed to be a superposition of an irrotational part $\vec{\nabla}\phi$, and a rotational component \vec{V}_w . The rotational component is attributed to the tip vortex shed from blade surfaces. Details on the calculation of \vec{V}_w are given later in Chapter III.

From the inviscid form of Bernoulli equation:

$$\phi_t + \frac{u^2 + v^2 + w^2}{2} + C_p T = \text{constant} \quad (2.50)$$

one can write the speed of sound as:

$$a^2 = (\gamma - 1)C_p T = a_\infty^2 - \frac{\gamma - 1}{2}[2\phi_t + u^2 + v^2 + w^2 - V_\infty^2] \quad (2.51)$$

Density is found from:

$$\frac{\rho}{\rho_\infty} = \left(\frac{a^2}{a_\infty^2} \right)^{1/\gamma - 1} \quad (2.52)$$

Equation (2.49), (2.51) and (2.52) may be combined to yield [92]:

$$\left(\frac{\rho}{a^2} \right) [\phi_{tt} + \phi_x \phi_{xt} + \phi_y \phi_{yt} + \phi_z \phi_{zt}] = [(\rho \phi_x)_x + (\rho \phi_y)_y + (\rho \phi_z)_z] + [(\rho u_w)_x + (\rho v_w)_y + (\rho w_w)_z] \quad (2.53)$$

where u_w , v_w and w_w are the x, y and z components of the rotational velocity field \vec{V}_w .

On a curvilinear coordinate system, the above equation may be written as:

$$\frac{\rho}{a^2 J} [\phi_{\tau\tau} + U\phi_{\xi\tau} + V\phi_{\eta\tau} + W\phi_{\zeta\tau}] = \left(\frac{\rho U}{J} \right)_{\xi} + \left(\frac{\rho V}{J} \right)_{\eta} + \left(\frac{\rho W}{J} \right)_{\zeta} + S \quad (2.54)$$

Detailed derivation of (2.51) and (2.52) are given by Sankar et al [86]. The term S is a function of grid motions and/or deformations [86]. The term vanishes for rigid grids and may be neglected for mildly deformed grids.

The contravariant velocity components U, V and W are:

$$\begin{aligned} U &= \xi_t + \phi_x \xi_x + \phi_y \xi_y + \phi_z \xi_z + u_w \xi_x + v_w \xi_y + w_w \xi_z \\ V &= \eta_t + \phi_x \eta_x + \phi_y \eta_y + \phi_z \eta_z + u_w \eta_x + v_w \eta_y + w_w \eta_z \\ W &= \zeta_t + \phi_x \zeta_x + \phi_y \zeta_y + \phi_z \zeta_z + u_w \zeta_x + v_w \zeta_y + w_w \zeta_z \end{aligned} \quad (2.55)$$

2.2.2 Numerical Discretization

As is the case in the Navier-Stokes equations, appropriate numerical approximations must be used to model the temporal and spatial derivatives contained in the potential flow equation. The following approach was used.

2.2.2.1 Temporal Discretization

As in the Navier-Stokes solver, a linearization procedure is necessary in order to solve the highly non-linear full-potential equation. Several terms are lagged by one time step, yielding a first order in time scheme. The linearized equation is given by:

$$\left(\frac{\rho}{a^2 J}\right)_{i,j,k}^{n+1} [\phi_{\tau\tau}^{n+1} + U^n \phi_{\xi\tau}^{n+1} + V^n \phi_{\eta\tau}^{n+1} + W^n \phi_{\zeta\tau}^{n+1}] = \left(\frac{\rho^n U^{n+1}}{J}\right)_{\xi} + \left(\frac{\rho^n V^{n+1}}{J}\right)_{\eta} + \left(\frac{\rho^n W^{n+1}}{J}\right)_{\zeta} \quad (2.56)$$

This equation was solved, as in the viscous region, by a time-marching scheme.

The term $\phi_{\tau\tau}$ is discretized by two-point backward difference scheme:

$$(\phi_{\tau\tau})_{i,j,k}^{n+1} = \frac{[(\phi^{n+1} - \phi^n) + (\phi^n - \phi^{n-1})]_{i,j,k}}{(\Delta t)^2} = \frac{[\Delta\phi^{n+1} - \Delta\phi^n]_{i,j,k}}{(\Delta t)^2} \quad (2.57)$$

where $\Delta\phi^{n+1} = \phi^{n+1} - \phi^n$

The mixed derivatives are evaluated by using upwind differencing for the spatial derivative and two-point backward differencing for the temporal derivative:

$$U(\phi_{\xi\tau})_{i,j,k}^{n+1} \cong \frac{U + |U|}{2\Delta t} \left[\frac{\Delta\phi_{i,j,k}^{n+1} - \Delta\phi_{i-1,j,k}^{n+1}}{\Delta\xi} \right] + \frac{U - |U|}{2\Delta t} \left[\frac{\Delta\phi_{i+1,j,k}^{n+1} - \Delta\phi_{i,j,k}^{n+1}}{\Delta\xi} \right] \quad (2.58)$$

The other spatial derivatives $V\phi_{\eta\tau}$ etc. were handled in a similar manner.

2.2.2.2 Spatial Discretization

The flux derivative terms such as $\left(\frac{\rho U}{J}\right)_{\xi}$ are computed with a two-point central difference formula:

$$\left[\left(\frac{\rho^n U^{n+1}}{J}\right)_{i,j,k}\right]_{\xi} = \frac{\left[\left(\frac{\rho^n U^{n+1}}{J}\right)_{i+1/2,j,k} - \left(\frac{\rho^n U^{n+1}}{J}\right)_{i-1/2,j,k}\right]}{\Delta\xi} \quad (2.59)$$

2.2.2.3 Upwind Differencing in Supersonic Region

In supersonic regions, the difference scheme must be biased in the direction of the flow as discussed by Murman and Cole [105]. In this work, the artificial compressibility method is used to bias the density in the direction of the flow if the flow is supersonic [106]:

$$\tilde{\rho}_{i+1/2,j,k} = \rho_{i+1/2,j,k} - \frac{(\rho q)_{i+1/2,j,k} - (\rho^* q^*)_{i-1/2,j,k}}{q_{i,j,k}} \quad (2.60)$$

where q is the flow speed $\sqrt{u^2 + v^2 + w^2}$, and ρ^* and q^* represent the density and velocity at the sonic point ($M=1$):

$$\begin{aligned}\frac{q^*}{q_\infty} &= \sqrt{\frac{2}{\gamma+1} \left(1 + \frac{\gamma-1}{2} M_\infty^2 \right)} \\ \frac{\rho^*}{\rho_\infty} &= \left(\frac{q^*}{q_\infty} \right)^{2/(\gamma-1)}\end{aligned}\quad (2.61)$$

Once the discretization and algebraic manipulation have been performed, the linearized full potential equation can finally be expressed [86] as:

$$\begin{aligned}a_{i,j,k}^n \Delta\phi_{i,j,k-1}^{n+1} + b_{i,j,k}^n \Delta\phi_{i,j-1,k}^{n+1} + c_{i,j,k}^n \Delta\phi_{i-1,j,k}^{n+1} + d_{i,j,k}^n \Delta\phi_{i,j,k}^{n+1} \\ + e_{i,j,k}^n \Delta\phi_{i+1,j,k}^{n+1} + f_{i,j,k}^n \Delta\phi_{i,j+1,k}^{n+1} + g_{i,j,k}^n \Delta\phi_{i,j,k+1}^{n+1} = R_{i,j,k}^n\end{aligned}\quad (2.62)$$

The individual elements of the coefficients are defined as:

$$\begin{aligned}a_{i,j,k} &= \left[\sigma_z \left(\frac{\rho W}{a^2 J \Delta t} \right)_{i,j,k}^n + \left(\frac{\rho A_6}{J} \right)_{i,j,k-1/2}^n \right] \\ b_{i,j,k} &= \left[\sigma_y \left(\frac{\rho V}{a^2 J \Delta t} \right)_{i,j,k}^n + \left(\frac{\rho A_4}{J} \right)_{i,j-1/2,k}^n \right] \\ c_{i,j,k} &= \left[\sigma_x \left(\frac{\rho U}{a^2 J \Delta t} \right)_{i,j,k}^n + \left(\frac{\rho A_1}{J} \right)_{i-1/2,j,k}^n \right]\end{aligned}$$

$$\begin{aligned}
d_{i,j,k} &= - \left[\left(\frac{\rho}{a^2 J \Delta t^2} \right)_{i,j,k}^n + \left(\frac{\rho U}{a^2 J \Delta t} \right)_{i,j,k}^n + \left(\frac{\rho V}{a^2 J \Delta t} \right)_{i,j,k}^n + \left(\frac{\rho W}{a^2 J \Delta t} \right)_{i,j,k}^n \right] \\
&\quad - \left[\left(\frac{\rho A_1}{J} \right)_{i+1/2,j,k}^n + \left(\frac{\rho A_1}{J} \right)_{i-1/2,j,k}^n + \left(\frac{\rho A_4}{J} \right)_{i,j+1/2,k}^n + \left(\frac{\rho A_4}{J} \right)_{i,j-1/2,k}^n \right] \\
&\quad - \left[\left(\frac{\rho A_6}{J} \right)_{i,j,k+1/2}^n + \left(\frac{\rho A_6}{J} \right)_{i,j,k-1/2}^n \right] \\
e_{i,j,k} &= \left[(1 - \sigma_x) \left(\frac{\rho U}{a^2 J \Delta t} \right)_{i,j,k}^n + \left(\frac{\rho A_1}{J} \right)_{i+1/2,j,k}^n \right] \\
f_{i,j,k} &= \left[(1 - \sigma_y) \left(\frac{\rho V}{a^2 J \Delta t} \right)_{i,j,k}^n + \left(\frac{\rho A_4}{J} \right)_{i,j+1/2,k}^n \right] \\
g_{i,j,k} &= \left[(1 - \sigma_z) \left(\frac{\rho W}{a^2 J \Delta t} \right)_{i,j,k}^n + \left(\frac{\rho A_6}{J} \right)_{i,j,k+1/2}^n \right] \\
R_{i,j,k} &= - \frac{1}{\Delta t^2} \left(\frac{\rho}{a^2 J} \right)_{i,j,k}^n \Delta \phi_{i,j,k}^n - \left(\frac{\rho U}{J} \right)_{i+1/2,j,k}^n + \left(\frac{\rho U}{J} \right)_{i-1/2,j,k}^n \\
&\quad - \left(\frac{\rho V}{J} \right)_{i,j+1/2,k}^n + \left(\frac{\rho V}{J} \right)_{i,j-1/2,k}^n - \left(\frac{\rho W}{J} \right)_{i,j,k+1/2}^n + \left(\frac{\rho W}{J} \right)_{i,j,k-1/2}^n
\end{aligned} \tag{2.63}$$

where:

$$\begin{aligned}
A_1 &= \xi_x^2 + \xi_y^2 + \xi_z^2 \\
A_4 &= \eta_x^2 + \eta_y^2 + \eta_z^2 \\
A_6 &= \zeta_x^2 + \zeta_y^2 + \zeta_z^2
\end{aligned}$$

The switching terms σ_x , σ_y , and σ_z arising from the upwind difference are defined as: $\sigma_x=0$ for $U>0$ and $\sigma_x=1$ for $U<0$, etc.

The matrix form of the equation (2.62) is:

$$[\mathbf{M}]\{\Delta\phi_{i,j,k}\}^{n+1} = \{\mathbf{R}_{i,j,k}\}^n \quad (2.64)$$

where \mathbf{M} is a septa-diagonal matrix. It would be computationally expensive to directly solve this large matrix equation. Therefore, a three factor approximate factorization scheme is employed.

$$[\mathbf{M}_1]d_{i,j,k}^{-1}[\mathbf{M}_2]d_{i,j,k}^{-1}[\mathbf{M}_3]\{\Delta\phi\}^{n+1} = \mathbf{R}_{i,j,k}^n \quad (2.65)$$

where

$$\begin{aligned} \mathbf{M}_1 &= d_{i,j,k} + c_{i,j,k}E_{\xi}^- + e_{i,j,k}E_{\xi}^+ \\ \mathbf{M}_2 &= d_{i,j,k} + b_{i,j,k}E_{\eta}^- + f_{i,j,k}E_{\eta}^+ \\ \mathbf{M}_3 &= d_{i,j,k} + a_{i,j,k}E_{\zeta}^- + g_{i,j,k}E_{\zeta}^+ \end{aligned} \quad (2.66)$$

The term E_{ξ}^{\pm} is a shift operator. For example:

$$E_{\xi}^{\pm}(\Delta\phi_{i,j,k}) = \Delta\phi_{i\pm 1,j,k} \quad (2.67)$$

Each of the matrices \mathbf{M}_1 , \mathbf{M}_2 , \mathbf{M}_3 are tridiagonal and are easily inverted:

$$\begin{aligned}
[\mathbf{M}_1] \Delta \phi^{**} &= \mathbf{R}^n \\
[\mathbf{M}_2] \Delta \phi^* &= d_{i,j,k} \Delta \phi^{**} \\
[\mathbf{M}_3] \Delta \phi^{n+1} &= d_{i,j,k} \Delta \phi^*
\end{aligned}
\tag{2.68}$$

Finally,

$$\phi^{n+1} = \phi^n + \Delta \phi^n
\tag{2.69}$$

2.3 Boundary and Interface Conditions

There are several surfaces surrounding the CFD domain, and there is also an interface surface between the full potential zone and the Navier-Stokes zone. The boundary conditions for these surfaces are discussed below. Figure 2.2 shows the boundaries of the computational domain, a multiblock grid system, where two block grids are generated around a single blade.

2.3.1 Navier-Stokes Zone

The inner zone extends from the rotor inboard boundary to the far field outboard boundary along the spanwise direction as shown in Figure 2.3. In the computational domain, the inner zone covers all the planes from $j=1$ plane to $j=j_{\max}$ plane in both the

upper and the lower block. In the chordwise direction, there are two interfaces corresponding to the upstream plane, $i=i_{match1}$, and the downstream plane, $i=i_{match2}$. The upper block and lower block are connected to each other at the block interface plane ($k=1$ for upper block, $k=k_{max}$ for lower block). The plane $k=k_{match}$ in each block corresponds to the interface between the inner zone and the outer zone in the normal direction. Adding another zonal interface in the spanwise direction does not give significant CPU time reduction, and was not pursued.

Figure 2.4 shows the partitioning of the computational domain for the inner zone and outer zone at a particular j plane in the radial direction. Figure 2.4 also illustrates the three interfaces ($i=i_{match1}$, $i=i_{match2}$, $k=k_{match}$) that surround the Navier-Stokes zone in each block. Boundary conditions are needed at these three interfaces to solve the governing equations.

For the Navier-Stokes region, the boundary conditions must be specified on the surrounding surfaces which include the blade surface, the surface between the two blocks, the blade inboard and outboard plane, and the interface surfaces.

At the blade surface, the no-slip condition is imposed for viscous flow:

$$\vec{v}_b = \vec{v}_{surface} = \vec{\Omega} \times \vec{r} - \vec{V}_{forwardflight} \quad (2.70)$$

The $\vec{\Omega} \times \vec{r}$ term takes into account the complex motion of the blade in forward flight, including pitching and flapping motions.

The pressure on the body surface is computed by solving the normal momentum equation $\partial p / \partial n = 0$.

It is difficult to set a physically based boundary condition for the inboard boundary near $r=0$. An extrapolation boundary condition is used at both the inboard and the outboard boundary. Errors at the inboard boundary affect the results only slightly due to the low dynamic pressures experienced in the inboard region.

At the connecting surface between the upper and lower block which is not on the blade surface, the flow values are averaged using values of the neighbor nodes in each block.

At the potential-flow/viscous-flow interfaces, the five components of the flow properties for Navier-Stokes equations are computed directly from the full-potential domain. The velocity components are found by adding potential and wake-induced velocities. For brevity, the formulation is given only for the interface $k=k_{match}$. A similar technique can be applied at the other two interfaces.

$$\begin{aligned}
 u_{i,j,k_{match+1}} &= (\phi_x)_{i,j,k_{match+1}} + u_w \\
 v_{i,j,k_{match+1}} &= (\phi_y)_{i,j,k_{match+1}} + v_w \\
 w_{i,j,k_{match+1}} &= (\phi_z)_{i,j,k_{match+1}} + w_w
 \end{aligned}
 \tag{2.71}$$

The density and energy are computed by the isentropic relations.

$$\frac{\rho}{\rho_{\infty}} = \left(\frac{a^2}{a_{\infty}^2} \right)^{1/\gamma-1}$$

$$e = \rho \left[\frac{a^2}{\gamma(\gamma-1)} + \frac{u^2 + v^2 + w^2}{2} \right] \quad (2.72)$$

where the local speed of sound can be determined by energy equation:

$$a^2 = a_{\infty}^2 + \frac{\gamma-1}{2} (V_{\infty}^2 - u^2 - v^2 - w^2 - 2\phi_t) \quad (2.73)$$

2.3.2 Full-Potential Zone

The boundary surfaces that need to be considered for the potential zone include the inboard boundary and the outboard boundary along spanwise direction, the upstream and downstream boundaries, and the interface surfaces. There is no need to handle the boundary conditions at the blade surface and wake sheet, which simplifies the procedure. Since the inboard root sections operate at low dynamic pressures, they contribute very little to the overall rotor performance. A linear extrapolation of the potential from the interior was found to be adequate at the inboard boundary $r=0$. At the connecting boundary shared between the upper and lower block, the velocity potential is averaged in the normal direction using the values of the neighbor surface in each block as:

$$\left(\phi_{i,j,1}\right)_{upper} = \left(\phi_{i,j,k \max}\right)_{lower} = \frac{\left(\phi_{i,j,2}\right)_{upper} + \left(\phi_{i,j,k \max-1}\right)_{lower}}{2} \quad (2.74)$$

The outboard boundary beyond the tip, the upstream and downstream boundaries, and the bottom and top boundaries are usually located far away from the rotor disk. The velocity potential is set to zero on these boundary surfaces which means that the velocity components are predominantly associated with the induced velocity \vec{V}_w . If the reflection of acoustic waves at the far field surfaces is a major concern, a non-reflective far-field boundary condition derived by Shankar et al [106] can be used.

The three interfaces are the same as those for inner zone. The interface conditions between the two zones must be carefully handled to allow three types of waves (acoustic, vorticity and entropy waves) to propagate from inner zone out to the far field without false reflections.

The entropy wave is ignored once it leaves the inner viscous zone, consistent with isentropic of potential flow assumptions. The vorticity is converted into vortex elements that are modeled using a Lagrangian wake model discussed later. The conservation of mass is accounted for by matching the normal component of velocity at the interface as:

$$v_n|_{NS} = v_n|_{FP} \quad (2.75)$$

which is equivalent to setting $\frac{W}{J}|_{NS} = \frac{W}{J}|_{FP}$ at the interface.

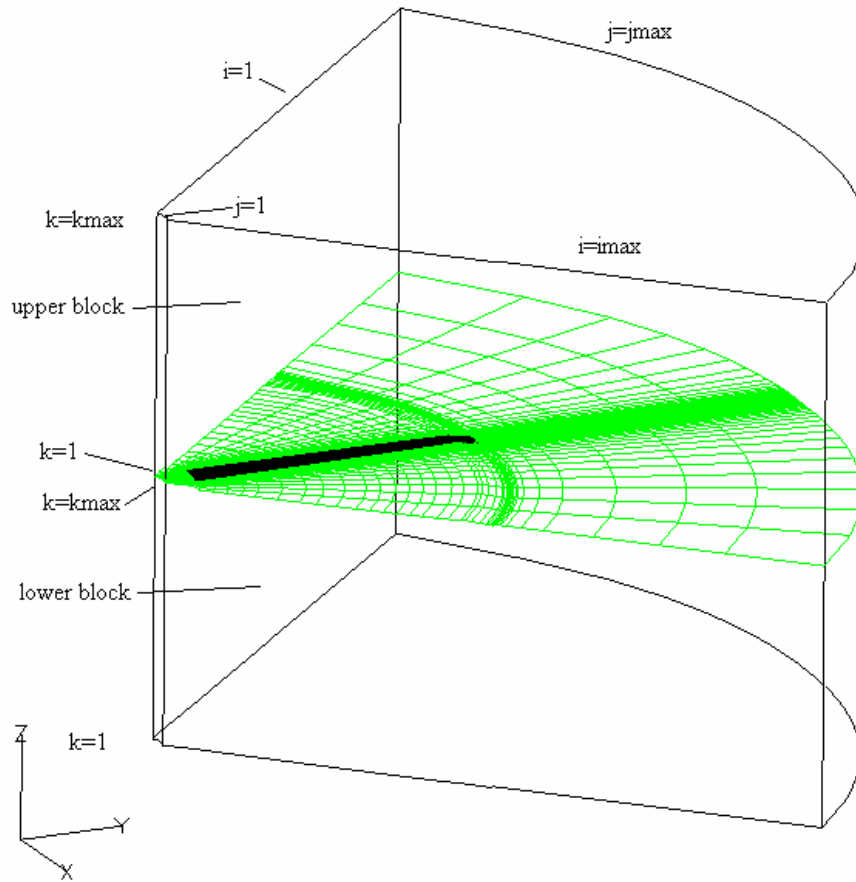


Figure 2.2: Multi-Block Boundary in the Computational Domain

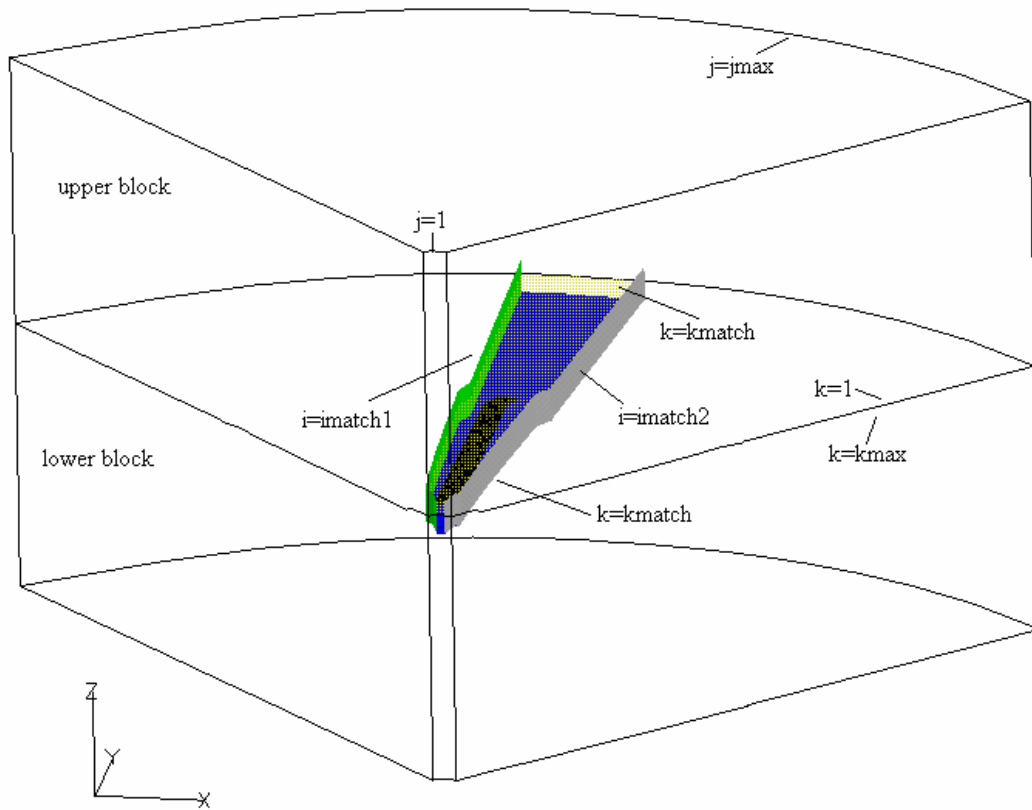
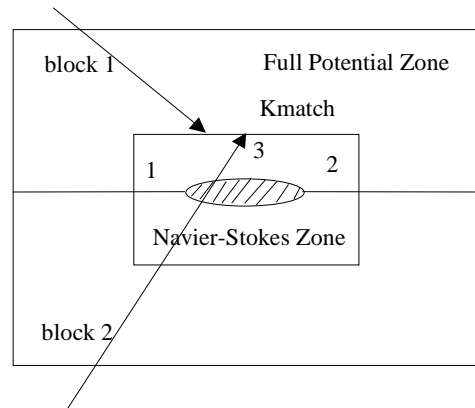


Figure 2.3: Flow Field Partition in the Computational Domain

$$\phi_n = (\vec{V}_{NS} - \vec{V}_{wake}) \cdot \vec{n}$$



$$\vec{V}_{NS} = \nabla \phi + \vec{V}_{wake}$$

Figure 2.4: Boundary Conditions at $j=\text{constant}$ Plane